

# Total CO<sub>2</sub> output and carbon origin discharged from Rincón de Parangueo Maar (México)

Mariana Patricia Jácome Paz<sup>a,\*</sup>, Claudio Inguaggiato<sup>b</sup>, Gilles Levresse<sup>c</sup>, Philippe Robidoux<sup>d</sup>, Hugo Delgado Granados<sup>a</sup>, Franco Tassi<sup>e</sup>

<sup>a</sup> Instituto de Geofísica, Universidad Nacional Autónoma de México, UNAM, Circuito Exterior s/n, Ciudad Universitaria, Delegación Coyoacán, C.P. 04510 Ciudad de México, Mexico

<sup>b</sup> Departamento de Geología, Centro de Investigación Científica y de Educación Superior de Ensenada (CICESE), Carretera Ensenada-Tijuana 3918, Ensenada, Baja California, Mexico

<sup>c</sup> Centro de Geociencias, Universidad Nacional Autónoma de México, UNAM, Blvd. Juriquilla 3001, Juriquilla La Mesa, 76230 Juriquilla, Querétaro, Mexico

<sup>d</sup> Centro de Excelencia en Geotermia de Los Andes - Plaza Ercilla, Santiago, Chile

<sup>e</sup> Scienze della Terra, Università di Firenze, Via La Pira, 4, 50121 Firenze, Italy

## ABSTRACT

A geochemical survey was carried out (May 2016) in the Rincón de Parangueo maar in Valle de Santiago, México. The challenge was to measure CO<sub>2</sub> and CH<sub>4</sub> fluxes discharged from soil and to investigate the chemical and isotopic compositions of interstitial soil gases and remaining vents at the bottom of maars system subjected to critical and high rate drawdown aquifer. Total CO<sub>2</sub> flux calculated by sequential Gaussian simulation is 10.6 ton d<sup>-1</sup> (± 2.1 ton d<sup>-1</sup>) over the entire crater maar area. Two degassing groups were recognized: Group A (background degassing) with values lower than 10 g m<sup>-2</sup> d<sup>-1</sup> (40% of the total measurements) and Group B with values ranging between 10 and 347.1 g m<sup>-2</sup> d<sup>-1</sup> (60% of the total amount of measurements). CH<sub>4</sub> flux ranges from 2.1 to 1577 g m<sup>-2</sup> d<sup>-1</sup>. CH<sub>4</sub>/CO<sub>2</sub> flux mean ratio is ~20.51 while CH<sub>4</sub>/CO<sub>2</sub> concentration ratios are 78 and 119 for bubbling gases and 8.4 for interstitial gases. The δ<sup>13</sup>C-CH<sub>4</sub> values are ~65 per mil vs V-PDB indicating a biogenic origin of methane in bubbling and interstitial gases. The δ<sup>13</sup>C-CO<sub>2</sub> values, ranging from -10.6 to -27.6 and -1.9 per mil vs V-PDB for bubbling gases and the interstitial gases, respectively, suggest secondary CO<sub>2</sub> consumption within the soil.

## 1. Introduction

Studies of diffuse degassing are fundamental to understand and to study volcanic and geothermal systems. The measurements of diffuse fluxes of CO<sub>2</sub> and CH<sub>4</sub> from soils and lakes in volcanic-hydrothermal systems are useful application to: (i) evaluate the budget of gases from different sources (total fluxes), (ii) monitor volcanic activity, (iii) understand the geological structure settings at local scale and (iv) estimate the energy released from the system (e.g. Allard et al., 1991; Giammanco et al., 1998; Chiodini et al., 2001; Hernández et al., 2001; Notsu et al., 2005; Mazot and Taran, 2009; Granieri et al., 2010; Burton et al., 2013; Italiano et al., 2014; Inguaggiato et al., 2012a, 2012b, 2013; Inguaggiato et al., 2017a, 2017b; Jácome-Paz et al., 2019; Peiffer et al., 2018). Among all these studies there are specific efforts to quantify the total global CO<sub>2</sub> released by subaerial volcanism, presenting the first global values of CO<sub>2</sub> flux from 79 to 65 Mt y<sup>-1</sup> (Gerlach and Gruber, 1985; Williams et al., 1992) to the last calculus of 300, 540 Mt y<sup>-1</sup> of CO<sub>2</sub> flux (Mörner and Etiope, 2002; Burton et al., 2013; Fisher, 2019 in that order). Following this global objective, it is

important contribute with more direct measurements of CO<sub>2</sub> flux in volcanic areas in order to better quantify the total global CO<sub>2</sub> and go to the insights of the role of volcanic sources as CO<sub>2</sub> producers. Advantageously, during direct measurement, not just the total carbon can be obtained, but also insights about the dynamic of carbon degassing in different volcanic environments.

To date, the carbon cycle in maar system is among the most complex hydrothermal-volcanic environments because depending on the chemistry of tephra deposits, post eruptive gases still released there and may be some effects on the chemistry of the local groundwater and the surrounding surface water (Ollier, 1967; Lorenz, 2007).

In maar systems not only CO<sub>2</sub> and its processes degassing have to be considered, also methane (CH<sub>4</sub>) is an important component of aquatic carbon cycling and CH<sub>4</sub> dynamics can represent a substantial proportion of the total carbon cycling in aquatic systems (Bastviken, 2009). Methanogenesis is the process of generation of methane by methanogens, which are anaerobic microorganisms or archaeons (Prescott et al., 1999). It is a dominant pathway for organic matter decomposition in many wetlands and flooded sediments due to the lack of oxidants

\* Corresponding author.

E-mail addresses: [jacome@igeofisica.unam.mx](mailto:jacome@igeofisica.unam.mx) (M.P. Jácome Paz), [inguaggiato@cicese.mx](mailto:inguaggiato@cicese.mx) (C. Inguaggiato), [hdg@igeofisica.unam.mx](mailto:hdg@igeofisica.unam.mx) (H. Delgado Granados), [franco.tassi@unifi.it](mailto:franco.tassi@unifi.it) (F. Tassi).

<https://doi.org/10.1016/j.jgexplo.2020.106558>

Received 3 March 2019; Received in revised form 31 March 2020; Accepted 24 April 2020

Available online 29 April 2020

0375-6742/ © 2020 Elsevier B.V. All rights reserved.

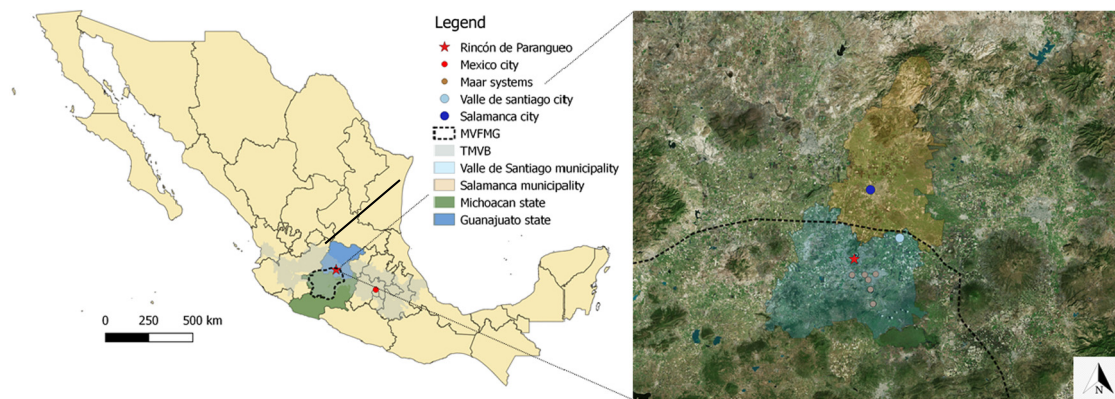


**Fig. 1.** Location of Rincón de Parangueo maar in the central part of Trans Mexican Volcanic Belt (TMVB). In the figure is indicated the boundary of the monogenetic volcanic field Michoacán–Guanajuato (MVFMG) and the maar systems around Rincón de Parangueo maar, as well as the municipalities and states mentioned in the text.

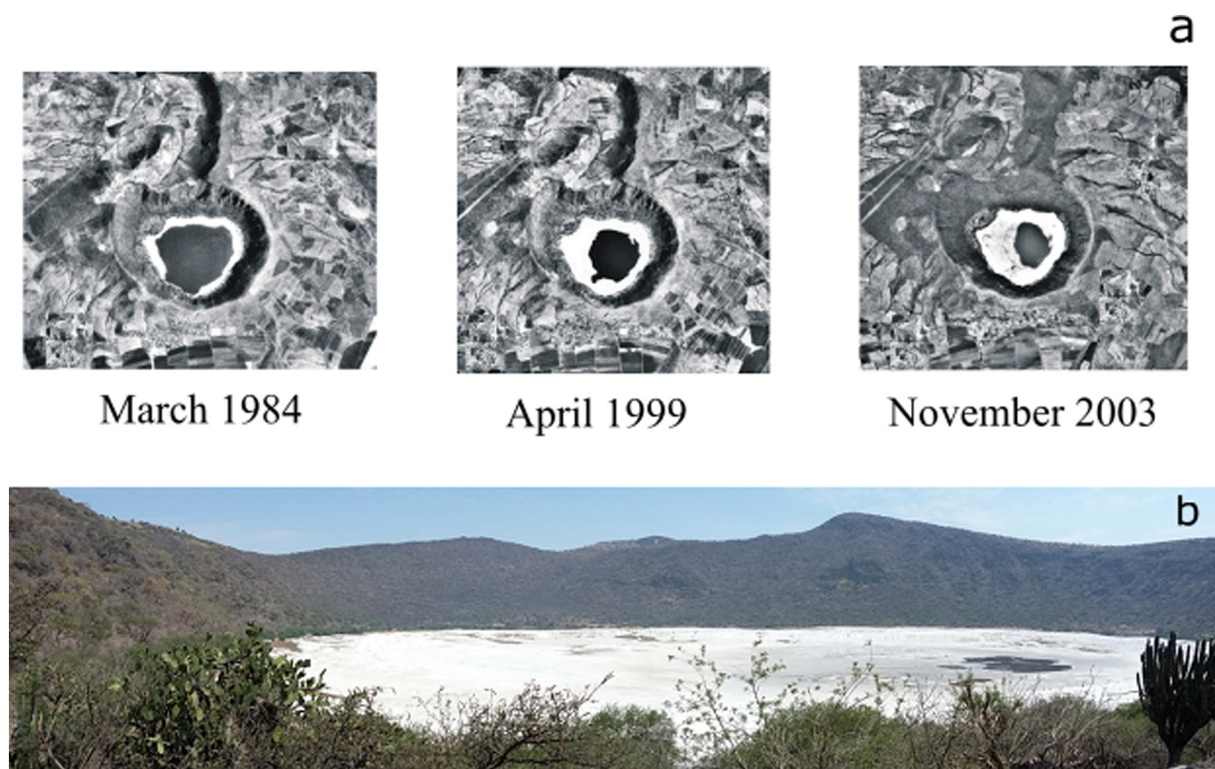


**Fig. 2.** a) Vertical air photos of the Rincón de Parangueo maar taken in three different dates (modified from [Aranda-Gómez et al., 2013](#)). Together with the evidence of dryness of lake, [Aranda-Gómez et al., 2013](#) also reported an active deformation occurring in the maar. b) View of maar crater during the fieldwork in May 2016.

typical of waterlogged soils. Methane can be produced according to different pathways in methanogenesis converting carbon dioxide, hydrogen, formate, acetate, and other compounds from organic matter of peat to methane ([Schlesinger and Bernhardt, 2013](#); [Flores, 2014](#)). Methanogens can convert (reduce) huge amounts of  $\text{CO}_2$  in  $\text{CH}_4$  in little time depending of pH and peat soil, their activity being usually optimum around neutrality conditions ([Flores, 2014](#)).

It is important to highlight that maar – diatreme volcanoes are the result of a phreatomagmatic eruption, within a monogenetic volcanic field. The phreatomagmatic eruption in subaerial environments is caused by the magma rises along a fissure and its interaction with groundwater ([Lorenz, 2007](#)). Therefore, water availability is a common factor in pre and post-eruptive dynamic of maar systems, resulting conditions for the post-eruptive existence of crater lakes or flooded crater sediments, environments propitious to the development of communities of anaerobic microorganisms.

Additionally, maar eruptions are characterized by short-lived, syn-eruptive hazards (e.g. earthquakes, eruption clouds, tephra fall, volcanic gases and rare reactivation ([Ollier, 1967](#); [Lorenz, 2007](#); [Nemeth et al., 2011](#); [Kshirsagar et al., 2015](#); [Nemeth and Kereszturi, 2015](#))). However, post-eruptive effects of maars are of great concern ([Lorenz, 2007](#)). According to [Lorenz \(2007\)](#), the short- and long-term post-eruptive studies must be focused in: i) quantification of the post-eruptive changes in shape, diameter and depth of crater, ii) possible subsidence of crater floor by compaction of diatreme fill, iii) studies of the re-establishment of the aquifers and the formation of crater lake, and finally iv) the release of juvenile gases.

Considering that the surroundings of maars are frequently near of large population centres, as is indicated in the spatial analysis of global maar distribution ([Graettinger, 2018](#)), one of the main challenge is to understand the main post-eruptive processes to reduce social, ecological and geological risks.



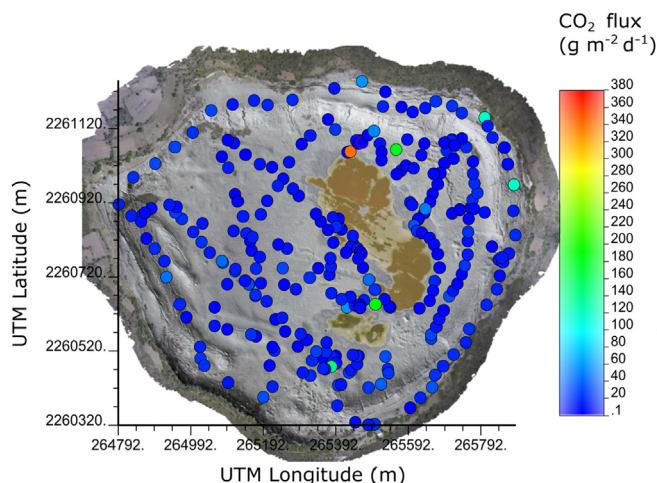


Fig. 3. Measured fluxes of  $\text{CO}_2$  with location over the entire maar area. Data are expressed in  $\text{g m}^{-2} \text{d}^{-1}$ .

Considering all information exposed above and even though maars are the second most common volcano type in subaerial environments (Lorenz, 2007), and contrary to many well-known maars systems worldwide considered as remaining carbon vent producers (e.g. Evans et al., 2009; Mazot et al., 2013; Andrade et al., 2019), the chemistry of degassing from maars systems found in Mexico are not well characterized. Therefore, maars in Mexico should be studied for diverse reasons, one of them is to characterize the emissions of gases and their origins to plan the best gas monitoring network able to detect the

variation of the emission rate of different gases in crater lakes, mainly  $\text{CO}_2$ ,  $\text{CH}_4$ ,  $\text{H}_2\text{S}$  (Kienle et al., 1980; Varekamp et al., 2000).

Before to set up a gas geochemical monitoring strategy, it is important to characterize chemically the gas emissions of the area and to identify the spatial distribution of main degassing sources. A full description of carbon-rich flux, origin releases and its transport still have not been well documented in the Rincón de Parangueo maar system.

Until the late 1980's, Rincón de Parangueo Maar was permanently filled with water. Under those circumstances, collecting gases and measuring carbon flux emissions did not represent a possible task. However, taking advantage of the almost complete desiccation state of the lake in 2016, the measurements of  $\text{CO}_2$  and  $\text{CH}_4$  fluxes diffused by soil could be performed easily over. The desiccation process in the lake environment may irreversibly affect the source and stationary chemical state of lake, therefore it will probably not recover from its original condition, so this study will set the baseline of carbon dynamic to monitor geochemically processes associated with desiccation of the lake and post-eruptive hazards.

This work represents the first gas geochemical characterization discharged from the Rincón de Parangueo Maar, mainly focused to: i) characterize the gas chemical composition, the origin of the fluids ii) calculate the total output of  $\text{CO}_2$  and iii) set the baseline for geochemical monitoring of gases.

## 2. Geological setting

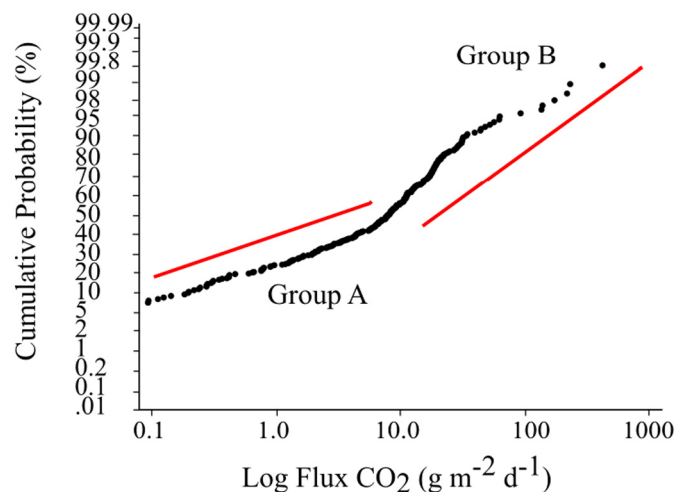
Rincón de Parangueo (RP) is a Quaternary maar located in the north-central part of the Trans Mexican Volcanic Belt (TMVB; Aranda-Gómez et al., 2002, 2009, 2010, 2013), on the central part of Mexico



Fig. 4. Fieldwork views. a) Sampling of interstitial gas, b) soil gas measurements with accumulation chamber method, c) view of some of the remnants of lake into the crater, d) example of remaining vent emitting gases where soil gases were sampled.

**Table 1**Main statistical parameters of measured CO<sub>2</sub> fluxes. There is an uncertainty of  $\pm 10\%$  for all data.

Number of points	Minimum (g m <sup>-2</sup> d <sup>-1</sup> )	Maximum (g m <sup>-2</sup> d <sup>-1</sup> )	Median (g m <sup>-2</sup> d <sup>-1</sup> )	Mean (g m <sup>-2</sup> d <sup>-1</sup> )	Standard deviation (g m <sup>-2</sup> d <sup>-1</sup> )
274	0.000	347.1	7.9	13.9	30.3

**Fig. 5.** Cumulated probability plot of CO<sub>2</sub> fluxes of Rincón de Parangueo maar.

(Fig. 1) northern of the Michoacán–Guanajuato Monogenetic Volcanic Field (MGMVF) and near of the Valle de Santiago (VS) town.

The cineritic cones and the maar of the VS are located approximately 100 km from the active volcanic front. Hasenaka and Carmichael (1985) report about 20 maar volcanoes in VS, which suggests a specific hydrological state for this portion of the MGMVF (Kshirsagar et al., 2015).

Quaternary magmas in the VS region are mildly alkaline and was interpreted as produced by mingling and mixing of subduction-related magmas of the TMVB and of intraplate magmas of the Northern Extensional Province of Mexico (Luhur et al., 2006; Aranda-Gómez et al., 2002).

In the VS area 50 cinder cones have been recognized, as well as 17 maar-type volcanoes and 15 lava shields (Aranda-Gómez et al., 2013). North and east VS town, there is a broad plain covered by alluvium, which probably represents the bottom of an extensive paleolake, i.e. Yuriria Lake, located 15 km south of VS (Aranda-Gómez et al., 2013).

RP maar is part of a volcanic complex formed chronologically by a continental lava shield, four maar-type volcanoes and a lava dome (Aranda-Gómez et al., 2010). Four of these volcanic bodies developed at or near a shield of continental lava of trachandesitic composition possibly since Pliocene (Murphy, 1986). Geochronology of RP is not precisely known but based on cross-cutting stratigraphic relationship it is younger than of the Santa Rosa tuff ring dated (next to the RP) at  $0.137 \pm 0.9$  Ma ( $^{40}\text{Ar}/^{39}\text{Ar}$ , groundmass concentrate; Aranda-Gómez et al., 2013).

### 2.1. Regional and local tectonic setting

The area between Querétaro and VS is located at the intersection of three regional fault systems: (Allard et al., 1991) Taxco–San Miguel de Allende (N20W), (Andrade et al., 2019) Chapala rift (N70E) and (Aranda-Gómez et al., 2002) El Bajío (N50W). All these structures showed Neogene or recent activity (e.g. Suter et al., 1995) and, together with the volcanic edifices, control the landscape in the region. The Chapala rift runs approximately ENE–WSW in the northern part of the MVFMG. Some of the medium sized volcanoes of the field are cut and offset by the normal faults (Hasenaka, 1992; Aranda-Gómez et al., 2013) of the rift. In addition to the ENE–WSW trend of normal faults, in

the northern portion of the MVFMG at least one N–S trending graben occurs (Aranda-Gómez et al., 2013).

Geophysical evidence showed that the Taxco–San Miguel Allende fault system is a major crustal discontinuity (Soler-Arrechalde and Urrutia-Fucugauchi, 1993; Urrutia-Fucugauchi et al., 1995; Arzate et al., 1999) that separates two segments in the TMVB with contrasting morphology and styles of volcanism. Caldera and lava dome complexes of intermediate to felsic composition and associated ignimbrites commonly occur east of the fault system. MVFMG and the broad plain known as El Bajío, on the downthrown side of the fault system, is locally interrupted by shield volcanoes and cinder cone and maar complexes.

Cinder cones around VS town define lineaments with two different orientations (N45W and N80E). The NW-trending alignments are likely to be related with Neogene normal faults exposed at the boundary between El Bajío and Sierra de Guanajuato, whereas the ENE-trending alignments are associated with an evident late Cenozoic normal fault system exposed south of Yuriria Lake.

### 2.2. Current state of Rincón de Parangueo crater

Inside the crater, the most prominent topographic feature is a 10–12 m high escarpment parallel to the old lake coast. The escarpment is produced by an annular shaped normal fault system (Aranda-Gómez et al., 2013). In the escarpment mass removal processes have been observed which mainly consist of rotational landslides in the eastern and northern portions of the escarpment and planar landslides to the west. Associated with rotational movements are roll-over folds and antithetical failures that produce small grabs near the main fault planes. Open folds and domes occur at the foot of the planar landslides in the western side of the desiccated lake.

Other impressive geological features are the calcareous platform and talus. The calcareous platform consists of oncolites, < 10 cm in diameter, and stromatolitic bioherms exposed near the edge of the inner scarp (Aranda-Gómez et al., 2013; Chacón et al., 2018). RP maar represents an important record of recent geological processes that reflects a dynamic interaction with microbial processes under increasingly extreme alkaline conditions (up to pH 10; Chacón et al., 2018). The observed soil and sediment deformations inside RP display a large number and variety of structures associated with ongoing active processes (Aranda-Gómez et al., 2013) caused by the large subsidence rate at the bottom of the maar, calculated at 50 cm/year (Carrera-Hernández et al., 2016).

The Valle de Santiago–Salamanca subsidence and piezometric level drawdown (highly populated zone) are related to the anthropogenic overexploiting regional aquifer (Fig. 2a; Aranda-Gómez et al., 2013). The desiccation of the RP Lake itself is almost complete (Fig. 2b) which may irreversibly affect the source and stationary chemical state of lake (e.g. carbon cycle in the water lake ecosystem).

RP lake has high neutralization degree pH  $\approx 10$ , and it is characterized by sodium-bicarbonate dominated water, with high ionic strength and the precipitation of the following minerals: halite, northupite, gaylussite, trona, natrite, eitelite, aragonite, hydromagnesite, and montmorillonite (Armienta et al., 2008; Aranda-Gómez et al., 2013). The high amounts of evaporite minerals and the dryness of the RP lake due to the progressive decrease of water volume highlights an active process of mass removal and salinity increase. Microbial activity is favoured by high salinity and it was recently characterized by Sánchez-Sánchez (2018) who described the large microbiological diversity



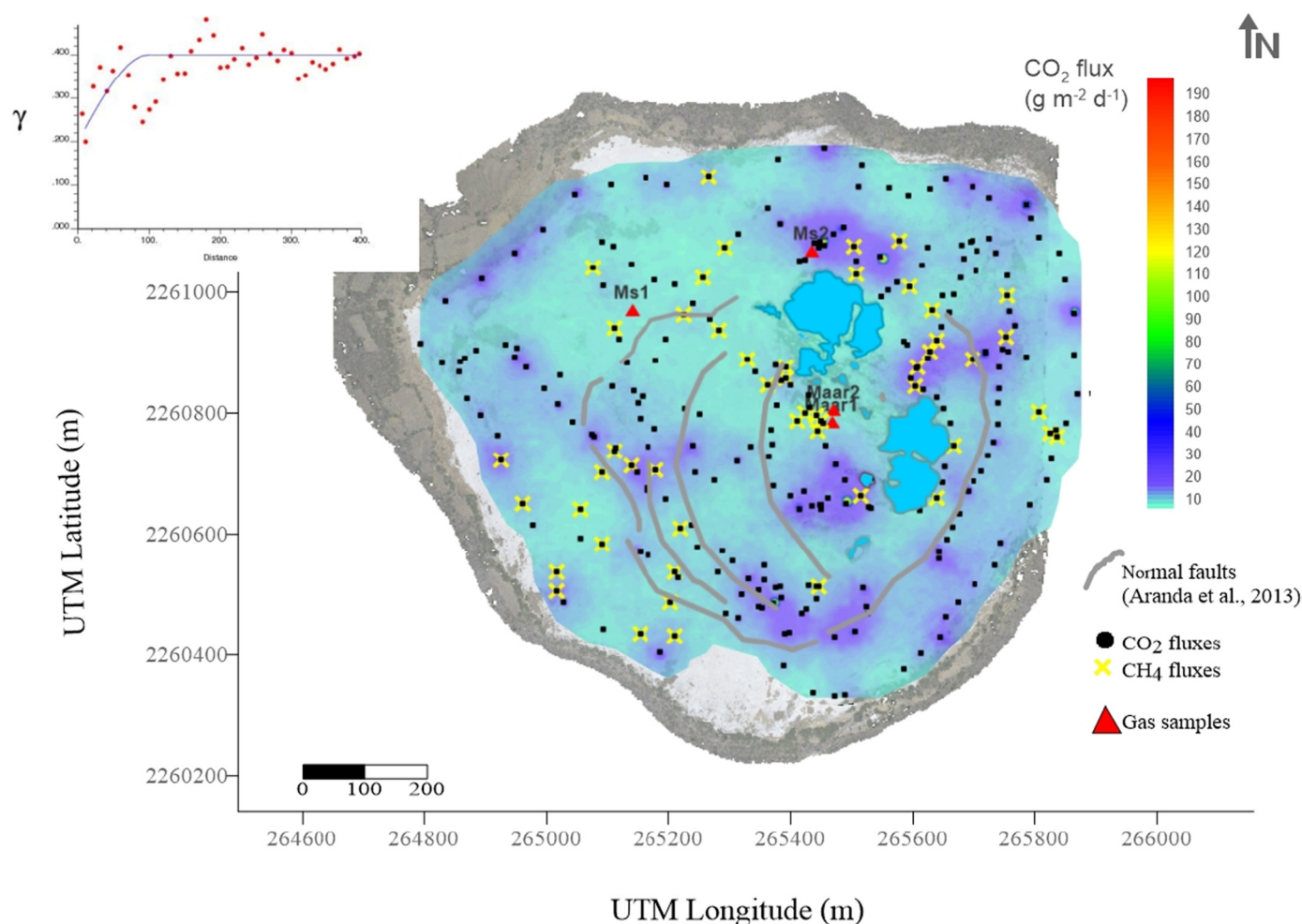


**Fig. 6.** The map shows the distribution of  $\text{CO}_2$  fluxes ( $\text{g m}^{-2} \text{d}^{-1}$ ). Location of gas samples are indicated by red triangles, measured points of  $\text{CO}_2$  flux by black dots and  $\text{CH}_4$  fluxes by yellow crosses. Normal faults inside the crater (taken from Aranda et al., 2008) and high values of diffuse emission measurements on this work have coincidences. The experimental variogram (red dots) and the theoretical variogram (solid line) used for the simulation are shown. (For interpretation of the references to color in this figure legend, the reader is referred to the web version of this article.)

**Table 2**

Main statistical parameters of Gaussian simulation results and total  $\text{CO}_2$  flux calculus.

Median ( $\text{g m}^{-2} \text{d}^{-1}$ ) ( $\pm 10\%$ )	$\text{T}\phi\text{CO}_2(\text{Median})$ ( $\text{ton d}^{-1}$ ) ( $\pm 10\%$ )	$\bar{x}$ ( $\text{g m}^{-2} \text{d}^{-1}$ ) ( $\pm 10\%$ )	$\text{T}\phi\text{CO}_2(\bar{x})$ ( $\text{ton d}^{-1}$ ) ( $\pm 20\%$ )	$\text{T}\phi\text{CO}_2(\text{GSA})$ ( $\text{ton d}^{-1}$ ) ( $\pm 1.9 \text{ ton d}^{-1}$ )	$\text{T}\phi\text{CO}_2(\text{SGS})$ ( $\text{ton d}^{-1}$ ) ( $\pm 2.1 \text{ ton d}^{-1}$ )
9.3	9.7	10.1	10.6	13.6	10.6

related to the laminated organo-sedimentary structures inside its crater, and specifically in the annular normal faults reported by Aranda-Gómez et al. (2013 and references therein)).

### 3. Materials and methods

In May 10th through May 12th 2016, during morning, 274 measurements of  $\text{CO}_2$  and  $\text{CH}_4$  fluxes ( $\phi\text{CO}_2$  and  $\phi\text{CH}_4$ , respectively) from the soil within the RP maar were carried out according to the accumulation chamber method (Fig. 3; Chiodini et al., 1998), using a West Systems flux meter equipped with: (Allard et al., 1991) LICOR LI-800, a nondispersive infrared  $\text{CO}_2$  sensor with detection range of 0.1 to 20,000 ppm, accuracy of  $< 3\%$  and reproducibility below 10% for the range 0.2 to 10,000  $\text{g m}^{-2} \text{d}^{-1}$ ; (Andrade et al., 2019) hydrocarbon flux detector  $\text{CH}_4$ -WS infrared (WS-HC IR), which has a flux detection range from 0.02 to 1444  $\text{g m}^{-2} \text{d}^{-1}$ , 5% accuracy, 2% of repeatability, 22 ppm resolution and  $\pm 25\%$  precision for the range

$-1.6$ – $80.2 \text{ g m}^{-2} \text{d}^{-1}$  and  $\pm 10\%$  precision for the range  $80.2$ – $2406 \text{ g m}^{-2} \text{d}^{-1}$ . Both, the LI-COR and WS-HC IR, are very stable detectors that allows the instrument to maintain its calibration for long periods (West Systems, 2012). At the time of data processing the instrumental uncertainty reported by the manufacturer was used.

Flux manager and flux Revision softwares, from West system®, were used to manage the field instrument and to check the data of the measured fluxes to obtain the correct main statistical parameters. Different groups of  $\phi\text{CO}_2$  and  $\phi\text{CH}_4$  values were recognized based on the graphical statistical approach (GSA, Sinclair, 1974; David, 1977), basically consisting on the evaluation of the main inflection points in the log  $\phi\text{CO}_2$  ( $\phi\text{CH}_4$ ) vs. cumulative probability plot.

The spatial distribution of the  $\phi\text{CO}_2$  and  $\phi\text{CH}_4$  values was computed by applying the sequential Gaussian simulation (SGS; Chiodini et al., 1998) with WinGslib software (Deutsch and Journel, 1998; Cardellini et al., 2003). One hundred simulations were carried out using a grid of  $10 \times 10 \text{ m}$ . Finally, after Gaussian simulation process, the total  $\text{CO}_2$

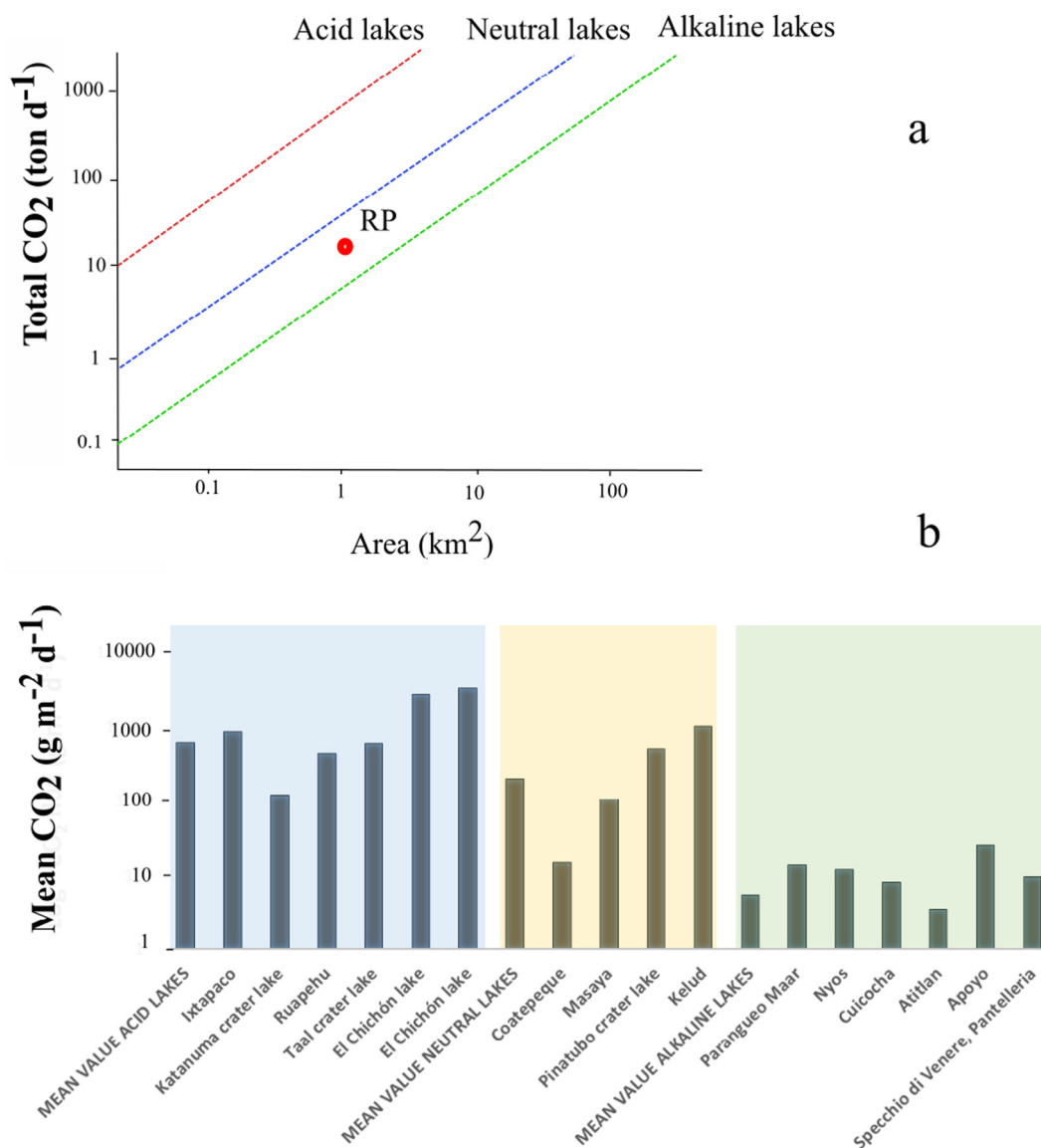


**Fig. 7.** a) Correlation between total CO<sub>2</sub> flux and crater lake area, subdivided as function of the pH: acidic lake, neutral lake, and alkaline lake (Modified from Mazot and Bernard, 2015; Inguaggiato et al., 2017b). b) Diverse values of CO<sub>2</sub> flux on crater and volcanic lakes are shown in the plot and classified according to pH. Mean values of neutral, acid and alkaline lakes and almost all values of lakes were taken from Perez et al. 2011. Values from El Chichón and Pantelleria lakes were taken from Jácome Paz et al., 2016a,b. Parangueo maar value is from this work.

**Table 3**

Main statistical values of CH<sub>4</sub> flux values.

Number of points	Minimum (g m <sup>-2</sup> d <sup>-1</sup> )	Maximum (g m <sup>-2</sup> d <sup>-1</sup> )	Median (g m <sup>-2</sup> d <sup>-1</sup> )	Mean (g m <sup>-2</sup> d <sup>-1</sup> )	Standard deviation (g m <sup>-2</sup> d <sup>-1</sup> )
52	2.1	1577.6	6.1	51.2	229.9

**Table 4**

Chemical and isotopic composition of gas samples (All results are in %Vol). n.d. no detection.

	CO <sub>2</sub>	N <sub>2</sub>	Ar	N <sub>2</sub> /Ar	O <sub>2</sub>	CH <sub>4</sub>	CH <sub>4</sub> /CO <sub>2</sub>	δ <sup>13</sup> C CO <sub>2</sub>	δ <sup>13</sup> C <sub>(CH<sub>4</sub>)</sub>	δD <sub>(CH<sub>4</sub>)</sub>
Maar 1	0.072	58.63	0.74	72.61	19.08	4.59	63.84	-10.61	-66.31	-202
Maar 2	0.14	56.75	0.77	60.33	15.87	19.84	141.71	-27.6	-67.43	-182
MS1	0.16	76.94	n.d.	78.17	20.61	0.0016	0.01	-0.99	n.d.	n.d.
MS2	0.12	79.45	1.04	76.94	19.93	1.28	10.67	-1.94	-64	-185

**Table 5**

Concentrations for hydrocarbons on Rincón de Parangueo samples. (All results are in %Vol).

	Ethane	Propane	Isobutane	Butane	Benzene
	C <sub>2</sub> H <sub>6</sub>	C <sub>3</sub> H <sub>8</sub>	iC <sub>4</sub> H <sub>10</sub>	nC <sub>4</sub> H <sub>10</sub>	C <sub>6</sub> H <sub>6</sub>
Maar 1	0.051	0.0044	0.00011	0.00013	0.0018
Maar 2	0.066	0.0047	0.00008	0.00009	0.0021
MS2	0.0048	0.00084	0.00002	0.00003	0.00014

and CH<sub>4</sub> outputs were reported in ton d<sup>-1</sup>.

Interstitial soil gases (Ms1 and Ms2) from the maar bottom were sampled by inserting a pipe in the soil at ~50 cm depth and using a syringe, silicon tube and a 3-way valve and then stored in 12 cc. pre-vacuum gas vials equipped with a rubber septum. Bubbling gases (Maar 1 and Maar 2) emitted from small hole of decametric size in a wet soil (Fig. 4) were sampled using an inverted funnel positioned above the bubbles that was connected to the same sampling line used for the collection of the interstitial gases.

The chemical composition of He, H<sub>2</sub>, N<sub>2</sub>, O<sub>2</sub>, CH<sub>4</sub>, CO<sub>2</sub>, and Ne was analysed at INGV-Palermo (Italy) by gas-chromatography Perkin Elmer Clarus 500 equipped with Carboxen 1000 columns, TCD and FID detectors. Analytical uncertainty was within ± 5%.

The <sup>13</sup>C/<sup>12</sup>C ratios in CO<sub>2</sub> and CH<sub>4</sub> (<sup>13</sup>C-CO<sub>2</sub> and <sup>13</sup>C-CH<sub>4</sub>, respectively), as well as the chemical composition of light hydrocarbons, were determined at University of Florence, Italy. The light hydrocarbons (C<sub>2</sub>-C<sub>4</sub> alkanes and C<sub>6</sub>H<sub>6</sub>) were analysed using a Shimadzu 14A GC equipped with a flame ionization detector (FID) and a 10 m long stainless-steel column filled with 23% SP 1700 on Chromosorb PAW (80/100 mesh). The <sup>13</sup>C-CO<sub>2</sub> values (expressed as ‰ vs. V-PDB) were determined using a Finnigan Delta plus XL mass spectrometer, after a two-step extraction and purification procedures of the gas mixtures by using liquid N<sub>2</sub> and a solid-liquid mixture of liquid N<sub>2</sub> and trichloroethylene (Evans et al., 1998). Internal (Carrara and San Vincenzo marbles) and international (NBS18 and NBS19) standards were used to estimate external precision. The analytical error and the reproducibility were ± 0.05‰ and ± 0.1‰, respectively. The <sup>13</sup>C/<sup>12</sup>C and <sup>2</sup>H/<sup>1</sup>H isotopic ratios in CH<sub>4</sub> (expressed as δ<sup>13</sup>C ‰ vs. V-PDB and δD ‰ vs. V-SMOW, respectively) were analysed by mass spectrometry (Varian MAT

250) according to the procedure by Schoell (1980). The analytical error was ± 0.15‰.

## 4. Results and discussion

### 4.1. $\phi$ CO<sub>2</sub> values

The  $\phi$ CO<sub>2</sub> values range from 0.01 to 347. 1 g m<sup>-2</sup> d<sup>-1</sup> (Table 1).

GSA technique was applied to the entire data set. The main inflection point in the cumulative probability plot separated in two groups the dataset. Group A (background degassing) consists of values lower than 10 g m<sup>-2</sup> d<sup>-1</sup> (40% of the measurements) while group B includes values included between 10 and 347. 1 g m<sup>-2</sup> d<sup>-1</sup> (60% of the measurements) (Fig. 5). Very few data (~2% of the measurements), have values higher than 100 g m<sup>-2</sup> d<sup>-1</sup>. The latter value usually indicates the highest value of ordinary soil respiration.

The mean value of group A is 1.7 g m<sup>-2</sup> d<sup>-1</sup> while the mean value of group B is 19.7 g m<sup>-2</sup> d<sup>-1</sup>. Considering the corresponding percentages of each degassing group ( $f_i$ ) multiplied by the total studied area (A) and the mean flux values ( $\bar{x}_i$ ) of each group (Eq. (1)), a total CO<sub>2</sub> flux ( $T\phi$ CO<sub>2</sub> (GSA)) of 13.6 ton d<sup>-1</sup> was obtained (± 1.9 ton d<sup>-1</sup>).

$$T\phi CO_{2(GSA)} = \sum_i A \bar{x}_i f_i \quad (1)$$

The SGS method was carried out with  $\phi$ CO<sub>2</sub> values ranging from 0.1 to 200 g m<sup>-2</sup> d<sup>-1</sup>. One outlier (347 g m<sup>-2</sup> d<sup>-1</sup>) was recognized and excluded of the data set before to implement the SGS method because the variogram obtained showed better correlation with distance without it, additionally, in the distribution map without outlier is more clear the spatial distribution, and the spatial alignments are highlighted (distribution map with outlier was made during analysis of data by the authors). The total flux was calculated using a spherical variogram model with a sill 0.4 and nugget of 0.2 (Fig. 6). The total area used for sequential Gaussian simulation was 1.0434 km<sup>2</sup>. The obtained distribution map suggests that the higher  $\phi$ CO<sub>2</sub> values (belonging to group B) have a concentric spatial distribution suggesting local structural control over the main degassing directions. The spatial structure of degassing expressed as main degassing paths coincide with the trace of the ring faults reported by Aranda-Gómez et al., 2013 (Fig. 6).

The total CO<sub>2</sub> flux (Table 2) calculated by Gaussian simulation

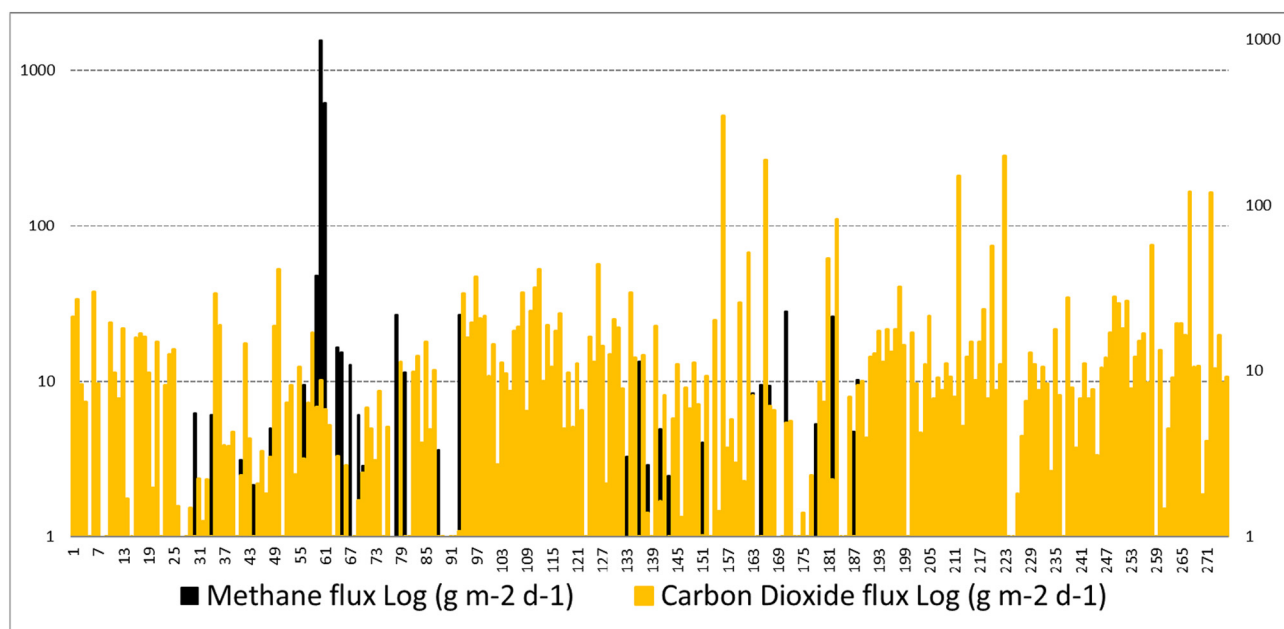


Fig. 8. Comparison between CH<sub>4</sub> and CO<sub>2</sub> fluxes in each measured point.

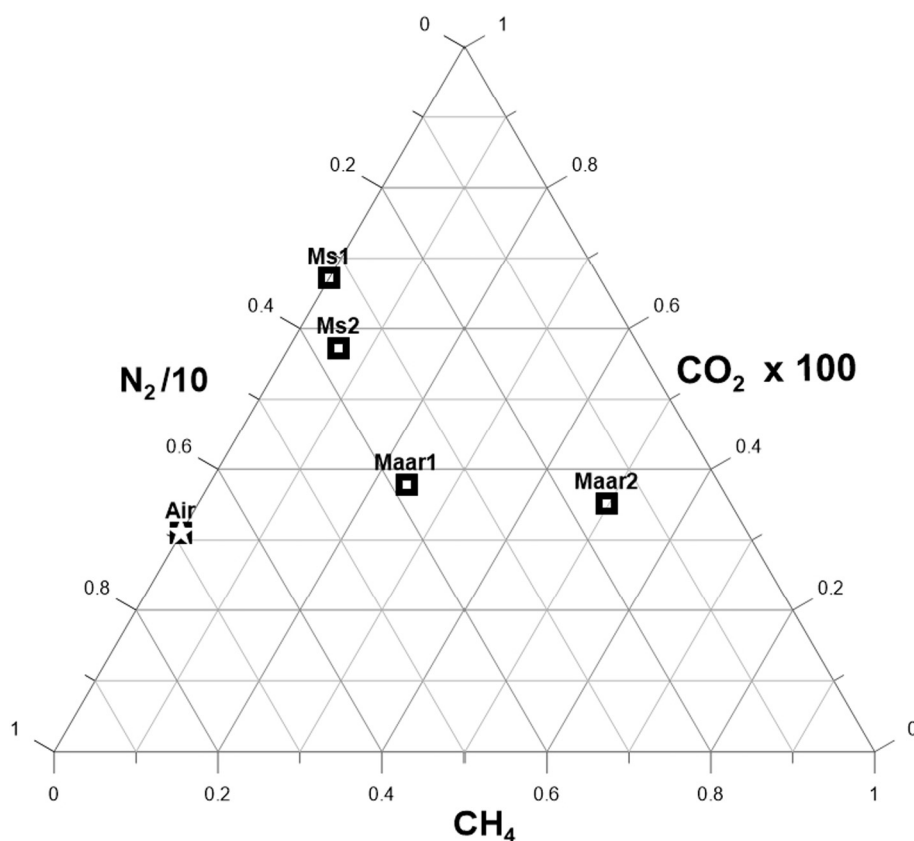


Fig. 9. Ternary diagram indicates the significant presence of methane in the Parangueo gas samples.

( $T\phi\text{CO}_2$  (SGS)) is  $10.6 \text{ ton d}^{-1} (\pm 2.1 \text{ ton d}^{-1})$ , lower than the  $T\phi\text{CO}_2$  (GSA). According to Cardellini et al. (2003), the total flow of GSA can be affected by several factors: (Allard et al., 1991) the division into the degassing groups represented with lognormal distributions are an approximation to the real phenomenon that may have a more complex distribution and (Andrade et al., 2019) the partitioning the dataset into groups is not unique. Because of this, GSA method is a tool to understand the degassing process associated in the study area, but  $T\phi\text{CO}_2$  (GSA) may not represent the most accurate result. Instead,  $T\phi\text{CO}_2$  (SGS) represents the preferred tool to total flux calculus because spatial variability of measurements is preserved (Goovaerts, 2001) and is the most used technique to calculate the total flux on soils (e.g. Cardellini et al., 2003; Inguaggiato et al., 2013; Jácome-Paz et al., 2019). As a comparison with other total fluxes, total mean flux ( $T\phi\text{CO}_2$  ( $\bar{x}$ )) and total median flux ( $T\phi\text{CO}_2$  (Median)) were calculated by multiply the total area for mean and median values, respectively, of dataset. These two total fluxes fall in the range of the uncertainty of  $T\phi\text{CO}_2$  (SGS).

With the complete lake desiccation, the presence of a possible sub-superficial aquifer of unknown pH can, at some point, control the magnitude of total  $\text{CO}_2$  flux degassing in the RP crater maar due to the  $\text{CO}_2$  absorption in water.

The total  $\text{CO}_2$  flux in Rincon de Parangueo Maar was compared with other outputs of  $\text{CO}_2$  flux measured around the world in volcanic lakes with variable pH according to the classification done by Mazot and Bernard (2015) and Inguaggiato et al. (2017a, 2017b). They were looking for the relation between total  $\text{CO}_2$  flux and area of different crater lakes, obtaining a clear statistical correlation (color lines in Fig. 7) between these two parameters as function of the pH: acidic lake, neutral lake and alkaline lake. Fig. 7(a) shows that even if the RP maar is almost dry in surface, the total  $\text{CO}_2$  flux value of the RP falls in the behaviour of an alkaline volcanic lake suggesting that degassing in RP maar still behaves as a lake. Additionally, taking the mean  $\text{CO}_2$  flux from Pérez et al. (2011) for different volcanic lakes and their

classification of those values according to pH, RP maar falls again in the alkaline lakes range (Fig. 7b). These classifications are evidence that the RP continues to degas as an alkaline lake, and this may be due to the presence of the sub-superficial aquifer with alkaline characteristics.

Armienta et al. (2008), reported high carbon concentration stored as carbonate minerals in the RP maar when crater Lake remained. The Lake had pH of 10.2, which caused all  $\text{CO}_2$  incoming as a flux to be absorbed in water. Because of this process (and interaction water/rock) carbon was stored as 40,000 mg/l of  $\text{CO}_3$  and 12,000 mg/l of  $\text{HCO}_3$  in the RP crater Lake instead be released totally as an efflux. It can be assumed for this residuary sub-superficial aquifer a similar pH value as the reported by Armienta et al. (2008) degassing as a shallow alkaline lake. Then, the drying process of this aquifer could release a considerable amount of carbon flux by losing the retention capacity of alkalinity/pH buffer while is drying.

#### 4.2. $\phi\text{CH}_4$ values

The 51 measured of  $\phi\text{CH}_4$  ranged from 2.1 to  $1577 \text{ g m}^{-2} \text{ d}^{-1}$  (Table 3). Their spatial distribution does not show anomalous degassing zones; and the values of fluxes are characterized by high variability showing not diffuse flux but focused emissions at some specific points. According to statistical analysis of data set and variogram, it is not convenient to elaborate a distribution map because there is not clear spatial correlation between measurements and there are not enough data to make a distribution map.

The range of ratios between  $\text{CH}_4$  and  $\text{CO}_2$  flux is  $\sim 0.03\text{--}335$ , and the mean  $\text{CH}_4/\text{CO}_2$  ratio is  $\sim 20.51$ . The large variability of this ratio indicates high methane emission in single points and lack of homogenous  $\text{CH}_4$  degassing. This spatial distribution suggests a biogenic component in the methane degassing.

The total  $\text{CH}_4$  output was calculated ( $T\phi\text{CH}_4$ ) considering (i) the same crater area used to calculate  $\text{CO}_2$  flux and (ii) the mean and



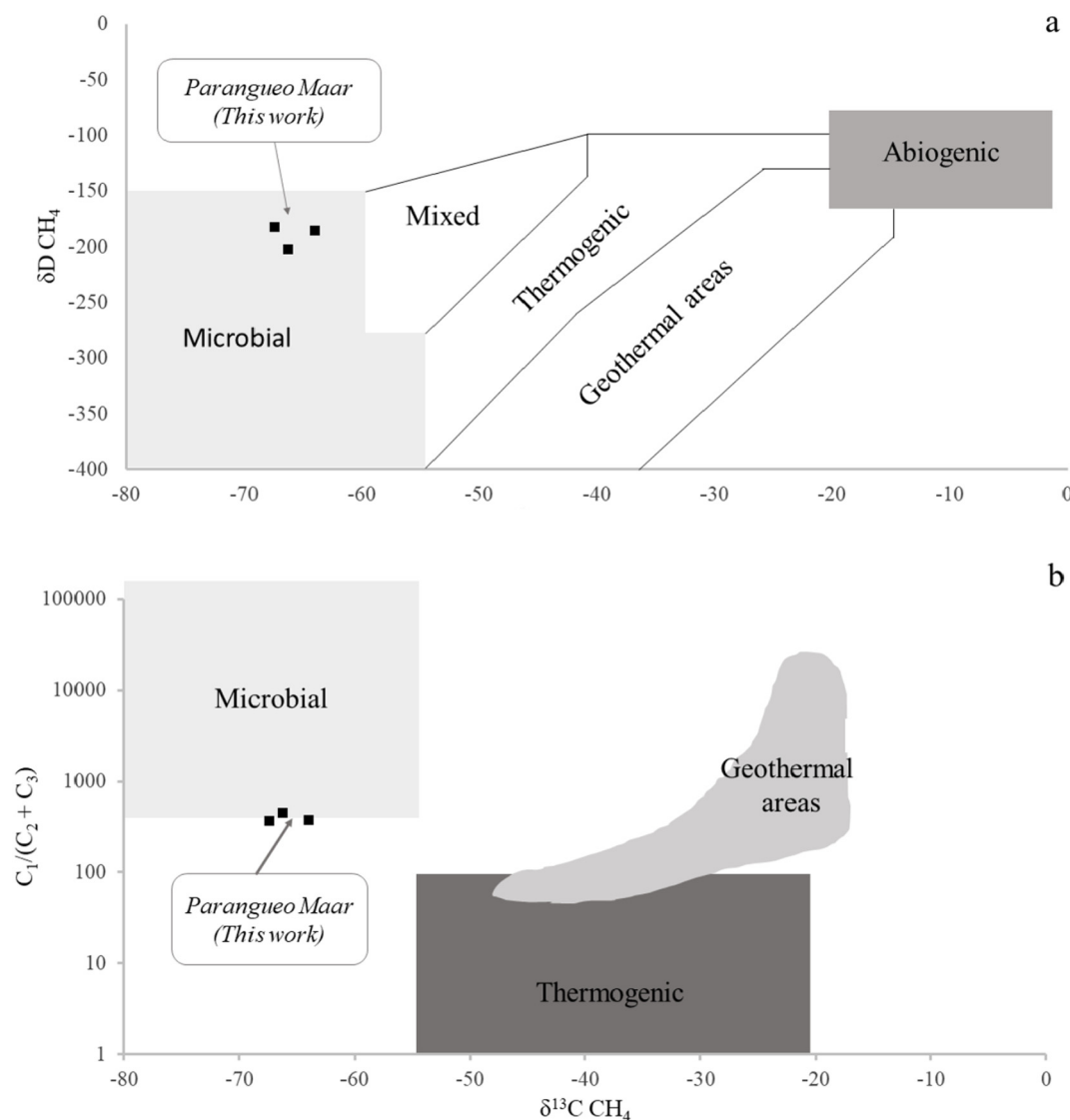


**Fig. 10.** a) By plotting the data of  $\delta^{13}C_{CH_4}$  vs. the  $\delta D_{CH_4}$ , the samples fall in the microbial field. b) The  $C_1/(C_2 + C_3)$  ratio coupled with  $\delta^{13}C_{CH_4}$  values for RP maar also indicate microbial origin of  $CH_4$ .

median measured values of  $CH_4$  flux. The obtained total fluxes are  $6.4 \text{ ton d}^{-1}$  for  $T\phi CH_{4(\text{Median})}$  value and  $53.4 \text{ ton d}^{-1}$  for  $T\phi CH_4 (\bar{x})$ .

#### 4.3. Chemical and isotopic gas composition

The chemical composition of gas indicates the presence of methane and light hydrocarbons (Tables 4 and 5).  $N_2$  and  $CO_2$  concentrations range from 56.45 to 79.45 and from 15.22 to 17.25 vol%, respectively. The  $N_2/O_2$  ratios are close to the ratio in the atmosphere, indicating that the samples were strongly affected by air contamination. The concentrations of  $CO_2$  and  $CH_4$  ranged from 0.16 to 0.35 and from 0.0016 to 26.28% vol, respectively. Fig. 8 shows that the gases emitted from the small hole of decametric size in the wet soil (Maar 1 and Maar 2 samples) are characterized by the highest methane concentrations. Methane is an important constituent of geothermal reservoirs, but its origin is somewhat controversial. Abiogenic and biogenic sources can be considered in geothermal fluids (D'Alessandro et al., 2009; Etiope and Sherwood Lowar, 2013). Thermal decomposition of organic matter at upper crust levels produces  $CH_4$  and light hydrocarbons, and usually this process is accompanied by a very high  $N_2/Ar$  ratio, because the degradation of organics produces  $N_2$  but not Ar (Taran and Gignenbach, 2003). RP samples gases show  $N_2/Ar$  ratio between 73 and 79 and high

contents of  $CH_4$ . As a comparison, the  $CH_4/CO_2$  concentration ratio is higher than the magmatic characteristic value (magmatic fluids at the surface should be characterized by  $CH_4/CO_2$  ratios  $< 10^{-6}$  (Giggenbach, 1997) suggesting a superficial origin of carbon gases (Fig. 9). Moreover, the low  $\delta^{13}C_{(CH_4)}$  isotope values of bubbling and interstitial gases (from  $-66$  to  $-64\text{‰}$ ) indicate a microbial origin. By plotting the  $\delta^{13}C_{CH_4}$  vs. the  $\delta D_{CH_4}$  and the  $CH_4/(C_2H_6 + C_3H_8)$  ratio values (also known as  $C_1/(C_2 + C_3)$  vs.  $\delta^{13}C_{CH_4}$  (e.g. D'Alessandro et al., 2009; and Yuce et al., 2014), a microbial origin of methane is confirmed (Fig. 10). In the case of  $CO_2$  isotopic composition, the  $\delta^{13}C(CO_2)$  values of  $-10.6$  and  $-27.6\text{‰}$  for bubbling gases and  $-1.9\text{‰}$  for interstitial gas, can suggest a mix between shallow processes (biogenic) and residual gas of a secondary process acting on  $CO_2$ . Methanogenesis can be an explanation for these isotopic values on surface and consistent with the relatively high  $CH_4$  concentrations.

Even when the isotopic signature allow us to know the predominantly microbial origin of  $CH_4$ , the total amount of  $CO_2$  and  $CH_4$  fluxes is comparable with active volcanic systems; this can be explained because high amount of  $CO_2$  is going up easily through the extensional cracking caused for the desiccation process and the tectonic structures into the crater. It can be inferred that ring normal faults may acting as the main diffuse degassing structures (DSS; Carapezza et al., 2009).

Then, CO<sub>2</sub> released favours the microbial activity allowing a high production of CH<sub>4</sub> by methanogenesis

## 5. Conclusions

A geochemical survey was carried out at the RP maar to characterize the soil  $\phi$ CO<sub>2</sub> and  $\phi$ CH<sub>4</sub> emissions and the chemical and isotope compositions of interstitial soil gases and bubbling gases. This study is a starting point to understand the carbon dynamic at RP maar and to quantify the CO<sub>2</sub> and CH<sub>4</sub> emissions to evaluate in the future possible changes on the flux gas output. The highest soil CO<sub>2</sub> flux measured at RP is 347 g m<sup>-2</sup> d<sup>-1</sup> and the total CO<sub>2</sub> flux obtained with Gaussian simulation is 10.6 ton d<sup>-1</sup>, comparable with degassing in shallow and alkaline crater lake.

The emission of CO<sub>2</sub> at Rincón de Parangueo crater shows a concentric distribution, according to the ring normal faults already identified by previous studies. High variability in CH<sub>4</sub>/CO<sub>2</sub> flux and concentration ratios could suggest strong influence of secondary process on these gases. Carbon and hydrogen isotope values indicate that methane has a microbial origin as well as while CO<sub>2</sub> is result of consumption process.

In summary, formation of high permeability zones due to the desiccation process and biogenic activity as sources of carbon compounds were recognized in the Rincón de Parangueo crater. Moreover, the drying process of the lake and the sub-superficial aquifer could increase the carbon flux emissions.

## CRedit authorship contribution statement

**Mariana Patricia Jácome Paz:** Conceptualization, Methodology, Writing - original draft. **Claudio Inguaggiato:** Conceptualization, Methodology. **Gilles Levresse:** Project administration, Resources, Validation, Conceptualization. **Philippe Robidoux:** Conceptualization, Methodology. **Hugo Delgado Granados:** Resources, Methodology, Writing - review & editing. **Franco Tassi:** Formal analysis, Methodology, Writing - review & editing.

## Declaration of competing interest

All authors declare that they have no financial and personal relationship with other persons or organizations that may improperly influence (skew) their work or state if there are no interests to declare.

## Acknowledgments

Authors thanks the private fund from Fluid cortical laboratory - CGEO, UNAM. The equipment used to measure soil gases was purchased with the mixed fund CONACYT-Government of the State of Veracruz. VER-2008-C02-109249. We are grateful to Dr. Salvatore Inguaggiato from INGV, Palermo, Italy for his field assistance and the Istituto Nazionale di Geofisica e Vulcanologia - Palermo (INGV) for the analytical support. We also thank the comments and suggestions by the editor, Prof. Stefano Albanese and two anonymous reviewers that greatly improve the original manuscript.

## References

Allard, P., Carbonelle, J., Dajlevic, D., Le Bronec, J., Morel, P., Robe, M.C., Maurenas, J.M., Faivre-Pierret, R., Martins, D., Sabroux, J.C., Zettwoog, P., 1991. Eruptive and diffuse emissions of CO<sub>2</sub> from Mount Etna. *Nature* 351, 387–391.

Andrade, C., Viveiros, F., Cruz, J.V., Branco, R., Moreno, L., Silva, C., Coutinho, R., Pacheco, J., 2019. Diffuse CO<sub>2</sub> flux emission in two maar crater lakes from São Miguel (Azores, Portugal). *J. Volcanol. Geotherm. Res.* 369, 188–202.

Aranda-Gómez, J.J., Housh, T.B., Luhr, J.F., Carrasco-Núñez, G., 2002. Geología de la región de Valle de Santiago (Guanajuato): Informe preliminar. *GEOS*. 22. pp. 392.

Aranda-Gómez, J.J., Chacón-Baca, E., Charles-Polo, M., Solorio-Munguía, J.G., Vega-González, M., Moreno-Arredondo, A., Origel-Gutiérrez, G., 2009. Collapse structures at the bottom of a recently desiccated maar lake: Rincón de Parangueo maar, Valle de

Santiago, México. In: IAVCEI 3rd International Maar Conference. 12. Asociación Geológica Argentina Publicaciones Especiales, Larguie, Argentina, pp. 3–4.

Aranda-Gómez, J.J., Levresse, G., Pacheco-Martínez, J., Ramos-Leal, J.A., Carrasco-Núñez, G., Chacón-Baca, E., González-Naranjo, G., Chávez-Cabello, G., Vega-González, M., Origel-Gutiérrez, G., Noyola-Medrano, C., 2010. Active subsidence at the bottom of a recently desiccated crater-lake and its environmental impact: Rincón de Parangueo, Guanajuato, México: Field trip guidebook. In: Eighth International Symposium on Land Subsidence: Querétaro, Qro. International Association of Hydrogeological Sciences, México, pp. 1–48.

Aranda-Gómez, J.J., Levresse, G., Pacheco-Martínez, J., Ramos-Leal, J.A., Carrasco-Núñez, G., Chacón-Baca, E., González-Naranjo, G., Chávez-Cabello, G., Vega-González, M., Origel, G., Noyola-Medrano, C., 2013. Active sinking at the bottom of the Rincón de Parangueo Maar (Guanajuato, México) and its probable relation with subsidence faults at Salamanca and Celaya. *Bol. Soc. Geol. Mex.* 65, 169–188.

Armienta, M.A., Vilaclara, G., De la Cruz-Reyna, S., Ramos, S., Cenicerio, N., Cruz, O., Aguayo, A., Arcega-Cabrera, F., 2008. Water chemistry of lakes related to active and inactive Mexican volcanoes. *J. Volcanol. Geotherm. Res.* 178, 249–258.

Arzate, J.A., Aguirre-Díaz, G.J., Arroyo, M., 1999. Mediciones geofísicas aplicadas al estudio de la falla Tarimoro-San Miguel Allende (SMA); una posible discontinuidad mayor en el basamento. 19. *GEOS*, pp. 237.

Bastviken, D., 2009. Encyclopedia of Inland Waters. pp. 783–805. <https://doi.org/10.1016/b978-012370626-3.00117-4>.

Burton, M.R., Sawyer, G.M., Granieri, D., 2013. Deep carbon emissions from volcanoes. *Rev. Mineral. Geochem.* 75, 323–354.

Carapezza, M.L., Ricci, T., Ranaldi, M., Tarchini, L., 2009. Active degassing structures of Stromboli and variations in diffuse CO<sub>2</sub> output related to the volcanic activity. *J. Volcanol. Geotherm. Res.* 82, 231–245.

Cardellini, C., Chiodini, G., Frondini, F., 2003. Application of stochastic simulation to CO<sub>2</sub> flux from soil: mapping and quantification of gas release. *J. Geophys. Res.* 108 (B9), 2425.

Carrera-Hernández, J.J., Levresse, G., Lacan, P., Aranda-Gómez, J.J., 2016. A low cost technique for development of ultra-high resolution topography: application to a dry maar's bottom. *Revista Mexicana de Ciencias Geológicas* 33 (1), 122–133.

Chacón, E., Aranda-Gómez, J.J., Charles-Polo, M., Sánchez-Ramos, M.A., Rivera-Muñoz, E., Levresse, G., Millán-Malo, B., 2018. Biohermal thrombolites from a crater lake in Rincón de Parangueo, Central Mexico. *South American Earth Sciences* 85, 236–249. <https://doi.org/10.1016/j.jsames.2018.04.013>.

Chiodini, G., Cioni, R., Guidi, M., Marini, L., Raco, B., 1998. Soil CO<sub>2</sub> measurements in volcanic and geothermal areas. *Appl. Geochem.* 13, 543–552.

Chiodini, G., Frondini, F., Cardellini, C., Granieri, D., Marini, L., Ventura, G., 2001. CO<sub>2</sub> degassing and energy release at Solfatara volcano, Campi Flegrei, Italy. *J. Geophys. Res.* 106 (B8), 16,213–16,221.

D'Alessandro, W., Bellomo, S., Brusca, L., Fiebig, J., Longo, M., Martelli, M., Pecoraino, G., Salerno, F., 2009. Hydrothermal methane fluxes from the soil at Pantelleria island (Italy). *J. Volcanol. Geotherm. Res.* 187, 147–157.

David, M., 1977. Geostatistical Ore Reserve Estimation. Elsevier Scientific Pub. Co., New York.

Deutsch, C.V., Journel, A.G., 1998. GSLIB: Geostatistical Software Library and Users Guide, 2nd ed. Oxford University Press, New York, pp. 369.

Etiopie, G., Sherwood Lowar, B., 2013. Abiotic methane on earth. *Rev. Geophys.* 51, 276–299.

Evans, W.C., White, L.D., Rapp, J.B., 1998. Geochemistry of some gases in hydrothermal fluids from the southern Juan de Fuca ridge. *J. Geophys. Res.* 15, 305–313.

Evans, W.C., Bergfeld, D., McGimsey, R.G., Hunt, A.G., 2009. Diffuse gas emissions at the Ukinrek Maars: Implications for magmatic degassing and volcanic monitoring. *Appl. Geochem.* 24, 527–535.

Fisher, Tobbias, et al., 2019. The emissions of CO<sub>2</sub> and other volatiles from the world's subaerial volcanoes. *Sci Rep* 9, 18716 (2019). Scientific Reports. doi:<https://doi.org/10.1038/s41598-019-54682-1>.

Flores, R.M., 2014. Chapter Origin of Coal as Gas Source and Reservoir Rocks in Coal and Coalbed Gas. <https://doi.org/10.1016/B978-0-12-396972-9.00003-3>.

Gerlach, T.M., Graber, E.J., 1985. Volatile budget of Kilauea volcano. *Nature* 313, 273–277.

Giammanco, S., Gurrieri, M., Valenza, S., 1998. Anomalous soil CO<sub>2</sub> degassing in relation to faults and eruptive fissures on Mount Etna (Sicily, Italy). *Bull. Volcanol.* 60, 252–259. <https://doi.org/10.1007/s004450050231>.

Giggenbach, W., 1997. Relative importance of thermodynamics and kinetic processes in governing the chemical and isotopic composition of carbon gases in high-heatflow sedimentary basins. *Geochim. Cosmochim. Acta* 61, 3763–3785.

Goovaerts, P., 2001. Geostatistical modeling of uncertainty in soil science. *Geoderma* 103 (1–2), 3–26.

Graettinger, A.H., 2018. Trends in maar size and shape using the global Maar Volcano Location and Shape (MaarVLS) database. *J. Volcanol. Geotherm. Res.* 357, 1–13. <https://doi.org/10.1016/j.jvolgeores.2018.04.002>.

Granieri, D., Avino, R., Chiodini, G., 2010. Carbon dioxide diffuse emission from the soil: ten years of observations at Vesuvio and Campi Flegrei (Pozzuoli), and linkages with volcanic activity. *Bull. Volcanol.* 72, 103–118. <https://doi.org/10.1007/s00445-009-0304-8>.

Hasenaka, T., 1992. Size, distribution and magma output rate for shield volcanoes of the Michoacán-Guanajuato volcanic field, central Mexico. In: Aoki, K.I. (Ed.), Subduction Volcanism and Tectonics of Western Mexican Volcanic Belt, Sendai, Japan. The Faculty of Science, Tohoku University, pp. 115–141.

Hasenaka, T., Carmichael, I.S.E., 1985. The cinder cones of the Michoacán-Guanajuato, central Mexico: their age, volume, and distribution, and magma discharge rate. *J. Volcanol. Geotherm. Res.* 25, 104–124.

Hernández, P.A., Notsu, K., Salazar, J.M., Mori, T., Natale, G., Okada, H., Virgili, G.,

- Shimoike, Y., Sato, M., Pérez, N.M., 2001. Carbon dioxide degassing by advective flow from Usu volcano, Japan. *Science* 292, 83–86.
- Inguaggiato, S., Calderone, L., Inguaggiato, C., Mazot, A., Morici, S., Vita, F., 2012a. Long-time variation of soil CO<sub>2</sub> fluxes at summit crater of Vulcano (Italy). *Bull. Volcanol.* 74, 1859–1863. <https://doi.org/10.1007/s00445-012-0637-6>.
- Inguaggiato, S., Mazot, A., Diliberto, S., Inguaggiato, C., Madonia, P., Rouwet, D., Vita, F., 2012b. Total CO<sub>2</sub> output from Vulcano Island (Aeolian Islands, Italy). *Geochim. Geophys. Res.* 13, 1–19. [https://doi.org/10.1029/2011GC003920\(Q02012\)](https://doi.org/10.1029/2011GC003920(Q02012)).
- Inguaggiato, S., Jácome Paz, M.P., Mazot, A., Delgado Granados, H., Inguaggiato, C., Vita, F., 2013. CO<sub>2</sub> output discharged from Stromboli Island (Italy). *Chem. Geol.* 339, 52–60. <https://doi.org/10.1016/j.chemgeo.2012.10.008>.
- Inguaggiato, C., Vita, F., Diliberto, I.S., Calderone, L., 2017a. The role of the aquifer in soil CO<sub>2</sub> degassing in volcanic peripheral areas: a case study of Stromboli island (Italy). *Chem. Geol.* 469, 110–116. <https://doi.org/10.1016/j.chemgeo.2016.12.017>.
- Inguaggiato, S., Cardellini, C., Taran, Y., Kalacheva, E., 2017b. The CO<sub>2</sub> flux from hydrothermal systems of the Karymsky volcanic Centre, Kamchatka. *J. Volcanol. Geotherm. Res.* 346, 1–9. <https://doi.org/10.1016/j.jvolgeores.2017.07.012>.
- Italiano, F., Yuce, G., Uysal, I.T., Gasparon, M., Morelli, G., 2014. Insights into mantle-type volatiles contribution from the dissolved gases in artesian waters of the Great Artesian Basin, Australia. *Chem. Geol.* 378–379, 75–88.
- Jácome Paz, M.P.J., Inguaggiato, S., Taran, Y., et al., 2016a. Carbon dioxide emissions from Specchio di Venere Lake. *Bull. Volcanol.* 78, 29. <https://doi.org/10.1007/s00445-016-1023-6>. Print ISSN 0258-8900 Online ISSN 1432-0819.
- Jácome Paz, M.P., Taran, Y., Inguaggiato, S., Collard, N., 2016b. CO<sub>2</sub> flux and chemistry of El Chichón Crater Lake (México) in the period 2013–2015: evidence for the enhanced volcano activity. *Geophysical Research Letters* 43, 127–134.
- Jácome-Paz, M.P., Pérez-Zárate, D., Prol-Ledesma, R.M., Rodríguez-Díaz, A.A., Estrada-Murillo, A.M., González-Romo, I.A., Magaña-Torres, E., 2019. Two new geothermal prospects in the Mexican Volcanic Belt: La Escalera and Agua Caliente-Tzitzio geothermal springs, Michoacán, México. *Geothermics* 80, 44–55. <https://doi.org/10.1016/j.geothermics.2019.02.004>.
- Kienle, J., Kyle, P.R., Self, S., Motyka, R.J., Lorenz, V., 1980. Ukinrek Maars, Alaska, I. April 1977 eruption sequence, petrology, and tectonic setting. *J. Volcanol. Geotherm. Res.* 7, 11–37.
- Kshirsagar, P.V., Siebe, C., Guilbault, M.N., Salinas, S., Layer, P.W., 2015. Late Pleistocene Alberca de Guadalupe mar volcano (Zacapu basin, Michoacán): stratigraphy, tectonic setting, and paleo – hydrogeological environment. *J. Volcanol. Geotherm. Res.* 304, 204–236.
- Lorenz, V., 2007. Syn – and post-eruptive hazards of maar-diatreme volcanoes. *J. Volcanol. Geotherm. Res.* 159, 285–312.
- Luhr, J.F., Kimberly, P., Siebert, L., Aranda-Gómez, J.J., Housh, T.B., Kysar, G., 2006. México's Quaternary Volcanic Rocks: Insights from the MEXPET Petrological and Geochemical Database: Geological Society of America Special Paper. 402. pp. 1–44.
- Mazot, A., Bernard, A., 2015. In: Rouwet, D. (Ed.), CO<sub>2</sub> Degassing From Volcanic Lakes in Volcanic Lakes, *Advances in Volcanology*, [https://doi.org/10.1007/978-3-642-36833-2\\_15](https://doi.org/10.1007/978-3-642-36833-2_15).
- Mazot, A., Taran, Y., 2009. CO<sub>2</sub> flux from volcanic Lake of El Chichón (Mexico). *Geofis. Int.* 48 (1), 73–83.
- Mazot, A., Smid, E.R., Schwendenmann, L., Delgado-Granados, H., Lindsay, J., 2013. Soil CO<sub>2</sub> flux baseline in an urban monogenetic volcanic field: the Auckland Volcanic Field, New Zealand. *Bull. Volcanol.* 75–757. <https://doi.org/10.1007/s00445-013-0757-7>.
- Mörner, N.A., Etiope, G., 2002. Carbon degassing from the lithosphere. *Global and Planetary Change*. 33. pp. 185–203. [https://doi.org/10.1016/S0921-8181\(02\)00070-X](https://doi.org/10.1016/S0921-8181(02)00070-X).
- Murphy, G.P., 1986. The chronology, pyroclastic stratigraphy, and petrology of the Valle de Santiago maar field, central Mexico. University of California, tesis de maestría, Berkeley, CA, U.S.A., pp. 55.
- Nemeth, K., Kereszturi, G., 2015. Monogenetic volcanism: personal views and discussion. *Int. J. Earth Sci.* 104, 2131–2146. <https://doi.org/10.1007/s00531-015-1243-6>.
- Nemeth, K., Haller, M.J., Siebe, C., 2011. Maars and scoria cones: the enigma of monogenetic volcanic fields. *J. Volcanol. Geotherm. Res.* 20, 1 (1–4), V–VIII.
- Notsu, K., Sugiyama, K., Uemura, A., Shomoike, Y., 2005. Diffuse CO<sub>2</sub> efflux from Iwojima volcano Izu-Ogasawara area, Japan. *Journal of Volcanology and Geothermal Research* 139, 147–161.
- Ollier, C.D., 1967. Maars. *Their Characteristics, Varieties and Definition*.
- Peiffer, L., Carrasco-Núñez, G., Mazot, A., Agnès, Villanueva-Estrada, R.E., Inguaggiato, C., Bernard Romero, R., Rocha Miller, R., Hernández Rojas, J., 2018. Soil degassing at the Los Hornos geothermal field (Mexico). *J. Volcanol. Geotherm. Res.* 356, 163–174. <https://doi.org/10.1016/j.jvolgeores.2018.03.001>.
- Pérez, N.M., Hernández, P.A., Padilla, G., Nolasco, D., Barrancos, J., Melán, G., Padrón, E., Dionis, S., Calvo, D., Rodríguez, F., Notsu, K., Mori, T., Kusakabe, M., Arpa, M.C., Reniva, P., Ibarra, M., 2011. Global CO<sub>2</sub> emission from volcanic lakes. *Geology* 39, 235–238.
- Prescott, L.M., Harley, J.P., Klein, D.A., 1999. Microbiology, 4th edn. WCB/McGraw-Hill, New York.
- Sánchez-Sánchez, J., 2018. Estromatolitos y comunidades microbianas en el cráter Maar Rincón de Parangueo y su relación con la geología. Tesis para obtener grado de maestría. Universidad Nacional Autónoma de México Online resource: [http://www.geociencias.unam.mx/geociencias/posgrado/tesis/maestria/sanchez\\_janet.pdf](http://www.geociencias.unam.mx/geociencias/posgrado/tesis/maestria/sanchez_janet.pdf).
- Schlesinger, W.H., Bernhardt, E.S., 2013. Chapter Wetland Ecosystems in *Biogeochemistry*, third edition. <https://doi.org/10.1016/B978-0-12-385874-0.00007-8>.
- Schoell, M., 1980. The hydrogen and carbon isotopic composition of methane from natural gases of various origins. *Geochim. Cosmochim. Acta* 44, 649–661.
- Sinclair, A.J., 1974. Selection of threshold values in geochemical data using probability graphs. *J. Geochem. Explor.* 3, 129–149.
- Soler-Arrechalde, A.M., Urrutia-Fucugauchi, J., 1993. The Querétaro-Taxco fracture system: a major NW-SE fault and crustal discontinuity in Central Mexico. 74. EOS, pp. 577.
- Suter, M., Quintero-Legorreta, O., López-Martínez, M., Aguirre-Díaz, G.J., Farrar, E., 1995. The Acambay graben: Active intraarc extension in the trans-Mexican volcanic belt. 14. Tectonics, Mexico, pp. 1245–1262.
- Taran, Y., Giggenbach, W., 2003. Geochemistry of Light Hydrocarbons in Subduction-related Volcanic and Hydrothermal Fluids. 10. Special Publication in Society of Economic Geologists, pp. 61–74.
- Urrutia-Fucugauchi, J., Soler-Arrechalde, A.M., Flores-Ruiz, J.M., 1995. Tectonics and volcanism in central Mexico -influence of pre- Neogene tectonics in the plate subduction-magmatic arc system. Geological Society of America Abstracts with programs 27, 189.
- Varekamp, J.C., Pasternack, G.B., Rowe, G.L., 2000. Volcanic lake systematics II. Chemical constraints. *J. Volcanol. Geotherm. Res.* 97, 161–180.
- West Systems, 2012. Portable Diffuse Flux Meter With LI-COR CO<sub>2</sub> Detector. Handbook. Italy, West Systems srl.
- Williams, S.N., Schaefer, S.J., Calvache, V.M.L., Lopez, D., 1992. Global carbon dioxide emission to the atmosphere by volcanoes. *Geochim. Cosmochim. Acta* 56, 1765–1770.
- Yuce, G., Italiano, F., D'Alessandro, W., Yalcin, T.H., Yasin, D.U., Gulbay, A.H., Ozyurt, N.N., Rojay, B., Karabacak, V., Bellomo, S., Brusca, L., Yang, T., Fu, C.C., Lai, C.W., Ozacar, A., Walia, V., 2014. Origin and interactions of fluids circulating over the Amik Basin (Hatay-Turkey) and relationships with the hydrologic, geologic and tectonic settings. *Chem. Geol.* 388, 23–39.